

# The homogeneity range and the microwave dielectric properties of the $\text{BaZn}_2\text{Ti}_4\text{O}_{11}$ ceramics

Anatolii G. Belous<sup>a</sup>, Oleg V. Ovchar<sup>a</sup>, Marjeta Macek-Krzmanc<sup>b</sup>, Matjaz Valant<sup>b,\*</sup>

<sup>a</sup> V.I. Vernadski Institute of General and Inorganic Chemistry, 03680 Kyiv, Ukraine

<sup>b</sup> Advanced Materials Department, Jozef Stefan Institute, 1000 Ljubljana, Slovenia

Received 20 April 2005; received in revised form 6 December 2005; accepted 9 December 2005

Available online 9 March 2006

## Abstract

Ceramics with a composition close to  $\text{BaZn}_2\text{Ti}_4\text{O}_{11}$  were synthesized according to various substitutional mechanisms in order to verify an existence of a homogeneity range in the vicinity of this composition. Structural and microstructural investigations showed that the crystal structure of  $\text{BaZn}_2\text{Ti}_4\text{O}_{11}$  was formed in the homogeneity range corresponding to the formula  $\text{BaZn}_{2-x}\text{Ti}_4\text{O}_{11-x}$  ( $0 < x < 0.1$ ). Densely sintered  $\text{BaZn}_{2-x}\text{Ti}_4\text{O}_{11-x}$  ( $0 < x < 0.1$ ) ceramics exhibited a dielectric constant around 30,  $\tau_f = -30$  ppm/K and high  $Q \times f$  values, which increased from  $\sim 68,000$  GHz at  $x = 0$  to  $\sim 83,000$  GHz at  $x = 0.05$ . Structurally, the deficiency of Zn in  $\text{BaZn}_{2-x}\text{Ti}_4\text{O}_{11-x}$  ( $0 < x < 0.1$ ) resulted in a slight decrease in the unit-cell volume. The influence of secondary phases in the  $\text{BaZn}_2\text{Ti}_4\text{O}_{11}$ -based materials on the microwave dielectric properties was also investigated. A presence of small amounts of ZnO,  $\text{BaTiO}_3$ , hollandite-type solid solutions ( $\text{Ba}_x\text{Zn}_x\text{Ti}_{8-x}\text{O}_{16}$ ) and  $\text{BaTi}_4\text{O}_9$  caused a decrease in  $Q \times f$  values.

© 2006 Elsevier Ltd. All rights reserved.

**Keywords:** X-ray methods; Dielectric properties; Powders-solid state reaction; Microwave dielectrics;  $\text{BaZn}_2\text{Ti}_4\text{O}_{11}$

## 1. Introduction

The crystal phase with the structure  $\text{BaZn}_2\text{Ti}_4\text{O}_{11}$  is present in various commercial microwave (MW) dielectric materials based on barium polytitanates ( $\text{BaTi}_4\text{O}_9$  and  $\text{Ba}_2\text{Ti}_9\text{O}_{20}$ ) doped with zinc, niobium, and tantalum oxides.<sup>1–3</sup> For this reason there has been a lot of interest in studying both its structure and its properties. The  $\text{BaZn}_2\text{Ti}_4\text{O}_{11}$  phase was synthesized for the first time by Gornikov et al.<sup>4</sup> using a high-temperature interaction between barium tetratitanate ( $\text{BaTi}_4\text{O}_9$ ) and zinc oxide (ZnO). The authors calculated the crystallographic parameters of the new compound, the composition of which they determined to be  $\text{Ba}_3\text{Zn}_7\text{Ti}_{12}\text{O}_{34}$  ( $3\text{BaTi}_4\text{O}_9 \times 7\text{ZnO}$ ).<sup>4</sup> This formula ( $\text{Ba}_3\text{Zn}_7\text{Ti}_{12}\text{O}_{34}$ ) was used for years by various authors of papers and patents when referring to the phase content of ceramics based on doped barium polytitanates.<sup>2–5</sup> More recently, in a paper by Roth et al.,<sup>6</sup> which is devoted to an investigation of the phase diagram of the ternary system  $\text{BaO}$ – $\text{ZnO}$ – $\text{TiO}_2$ , the authors reported the chemical composition of the compound

found in Ref. 4 to be  $\text{BaZn}_2\text{Ti}_4\text{O}_{11}$ , with the ratio of the starting oxides being close to 1:2:4. According to the results of Ref. 6, the crystal structure of  $\text{BaZn}_2\text{Ti}_4\text{O}_{11}$  is formed by a three-dimensional framework of distorted octahedra, shared by common edges and corners. In the crystal lattice of  $\text{BaZn}_2\text{Ti}_4\text{O}_{11}$  the Ti atoms occupy only the octahedral sites, whereas the Zn atoms can reside at both the tetrahedral and octahedral interstices.<sup>6</sup> Each unit cell comprises a total of 8  $\text{ZnO}_4$ , 8  $\text{ZnO}_6$ , and 32  $\text{TiO}_6$  units, with no  $\text{ZnO}_4$  and  $\text{ZnO}_6$  polyhedra sharing common edges and corners. Since both Zn and Ti atoms occupy the octahedral sites there is a possibility of their partial mutual substitution. This was also mentioned in Ref. 6. Moreover, the  $\text{BaZn}_2\text{Ti}_4\text{O}_{11}$  structure allows the existence of both cation and anion vacancies. These data suggest the possibility of the existence of a certain homogeneity range for the  $\text{BaZn}_2\text{Ti}_4\text{O}_{11}$  compound in the vicinity of its stoichiometric composition 1:2:4. This means that the exact composition can deviate from the formula  $\text{BaZn}_2\text{Ti}_4\text{O}_{11}$ . In spite of this the notation “124” phase is used throughout this text for every phase with a composition close to  $\text{BaZn}_2\text{Ti}_4\text{O}_{11}$ , except for the single-phase materials where the exact composition is known. However, this fact has not yet been confirmed experimentally. It should be noted that when formed, the variation of the chemical composition within the homogeneity range

\* Corresponding author.

E-mail address: [m.valant@lsbu.ac.uk](mailto:m.valant@lsbu.ac.uk) (M. Valant).

can affect the dielectric properties drastically. For instance, in barium lanthanide titanate,  $\text{Ba}_{6-x}\text{Ln}_{8+2x/3}\text{Ti}_{18}\text{O}_{54}$ , the mutual substitution of Ba and Ln atoms in the homogeneity region  $0 \leq x \leq 3$  results in changes in the permittivity ( $\epsilon$ ) by 20–30%, while the dielectric loss tangent ( $\tan \delta$ ) changes by 2–3 times.<sup>7</sup> However, there is no published data on the electrophysical properties of the  $\text{BaZn}_2\text{Ti}_4\text{O}_{11}$  compound. It is only reported that this phase displays a positive temperature coefficient of permittivity ( $\tau_\epsilon$ ) in the MW region, and could therefore be utilized as a secondary phase for the development of temperature-stable dielectric ceramics based on  $\text{BaTi}_4\text{O}_9$  in order to compensate for this compound's negative  $\tau_\epsilon$ .<sup>6</sup> The absence of MW data related to the  $\text{BaZn}_2\text{Ti}_4\text{O}_{11}$  compound does not allow us to correctly interpret the microwave parameters of materials based on barium polytitanates, and as a result to optimize the composition of current, commercial MW ceramics. In addition, in order to successfully predict the properties of materials based on the  $\text{BaO-ZnO-TiO}_2$  ternary system the phase diagram reported by Roth et al. should be supplemented with new data relating to the partial solid solubility of  $\text{TiO}_2$  in  $\text{Zn}_2\text{TiO}_4$  ( $\text{Zn}_2\text{TiO}_4 + x\text{TiO}_2$  ( $0.0 \leq x \leq 0.33$ )).<sup>8</sup> This type of solid solution is denoted in the remainder of the text as  $\text{Zn}_2\text{TiO}_4$  ss. It was stated previously that in the  $\text{ZnO-TiO}_2$  binary system only  $\text{Zn}_2\text{TiO}_4$  is supposed to be stable at high temperatures.<sup>9</sup>

The aim of this study was to investigate the effect of chemical composition and sintering conditions on the structural stability of  $\text{BaZn}_2\text{Ti}_4\text{O}_{11}$  as well as on its dielectric properties in the MW region.

## 2. Experimental

The powders for producing the polycrystalline materials investigated in this study were synthesized using a solid-state reaction technique. All the materials were produced in a two-stage process. In the first stage the following precursors were synthesized: barium polytitanates ( $\text{Ba}_4\text{Ti}_{13}\text{O}_{30}$ ,  $\text{BaTi}_4\text{O}_9$ ,  $\text{BaTi}_5\text{O}_{11}$ ) and solid solutions based on  $\text{Zn}_2\text{TiO}_4$ . High-purity  $\text{BaCO}_3$ ,  $\text{ZnO}$  and  $\text{TiO}_2$  were used as the starting reagents. The mixing and grinding of the starting reagents, in appropriate quantities, was carried out in ball mills for 8 h. The resulting mixtures were then dried at  $150^\circ\text{C}$ , calcined at  $1150\text{--}1200^\circ\text{C}$  for 4 h, and then homogenized. During the second stage the synthesized precursors were mixed in appropriate ratios and ball milled for 4–8 h. The dried powders with added binder were then pressed into disc-shaped pellets. The temperature treatment of the pressed pellets was carried out at temperatures in the range  $800\text{--}1250^\circ\text{C}$  for 4 h. The phase composition of the samples after the heat treatment was determined by X-ray diffraction using a “DRON 4” diffractometer with  $\text{Cu K}\alpha$  radiation. The X-ray powder-diffraction studies for determining the unit-cell parameters were performed with a Bruker AXS D4 Endeavor diffractometer using  $\text{Cu K}\alpha$  radiation. The X-ray powder-diffraction data were collected from  $15^\circ < 2\theta < 80^\circ$  with a step of  $0.02^\circ$ , a counting time of 10 s, and a variable V6 slit. The DIFFRAC plus TOPAS R program was used to determine the lattice parameters of the  $\text{BaZn}_{2-x}\text{Ti}_4\text{O}_{11-x}$  ( $0 \leq x \leq 0.05$ ).

The microstructural studies of the samples were conducted with a scanning electron microscope (SEM) (Model JXA 840A, JEOL, Tokyo, Japan) coupled with an energy-dispersive X-ray spectrometer (EDX) and appropriate software (Series II X-ray microanalyzer, Tracor Northerm, Middleton, WI).

The dielectric properties of the ceramic samples were measured at frequencies of 6–12 GHz with the dielectric-resonator method using both the cavity-reflection technique and transmission waveguide analysis. In the former case the dielectric losses of the materials ( $\tan \delta$ ) were calculated from the frequency dependence of the transmission coefficient in the vicinity of the resonant frequency ( $f_{\text{res}}$ ). The temperature dependencies of the permittivity were calculated from the temperature dependencies of  $f_{\text{res}}$ . The dielectric characteristics of the materials,  $\epsilon$ ,  $Q$ , and  $\tau_f$ , at frequencies around 10 GHz were examined using a modified dielectric-resonator method on an appropriate disk sample placed in the isolated waveguide section. The magnitudes of the  $Q$ -factors were additionally measured by means of the cavity-reflection method using a Network Analyzer HP 8719C (50 MHz–13.5 GHz).

## 3. Results and discussion

### 3.1. Homogeneity range of the $\text{BaZn}_2\text{Ti}_4\text{O}_{11}$ compound

The crystal structure of  $\text{BaZn}_2\text{Ti}_4\text{O}_{11}$ , determined by Roth et al.,<sup>6</sup> assumes several crystallographic features that can result in the existence of a certain homogeneity range. Therefore, in order to determine the correct compositional ranges corresponding to the phase stability we investigated several schemes for possible substitutional mechanisms (Fig. 1).

#### 3.1.1. Scheme $\text{BaZn}_{2-2x}\text{Ti}_{4+x}\text{O}_{11}$ (substitutional mechanism 1)

This scheme involves the substitution of one Ti atom for two Zn atoms for  $x > 0$ , and vice versa for  $x < 0$ . In the former case the substitutional formula fits well with the crystal-structure features determined by Roth et al.<sup>6</sup>: with an increase in  $x$  the total number of oxygen atoms remains unchanged for the unit cell of the

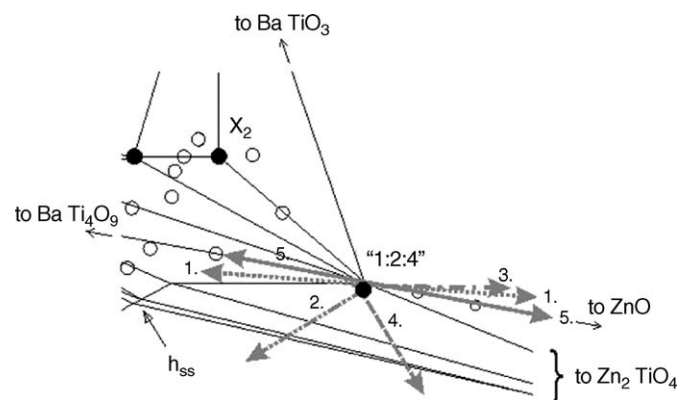


Fig. 1. Schematic representation of the tested substitutional mechanisms (extracted from the phase diagram reported by Roth et al.<sup>6</sup>)  $X_2 \rightarrow \text{Ba}_4(\text{Zn}_2\text{Ti}_{10})\text{O}_{26}$ , hss  $\rightarrow$  hollandite-type  $\text{Ba}_x\text{Zn}_x\text{Ti}_{8-x}\text{O}_{18}$  solid solution.

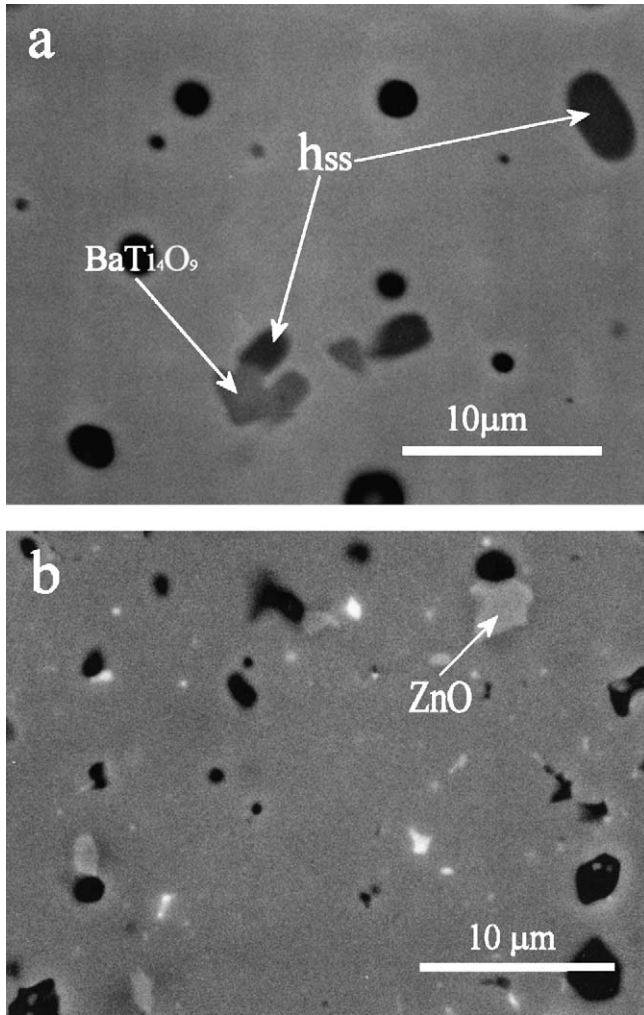


Fig. 2. SEM micrographs of the  $\text{BaZn}_{2-2x}\text{Ti}_{4+x}\text{O}_{11}$  ceramics for  $x=0.05$  (a),  $x=-0.1$  (b).

$\text{BaZn}_2\text{Ti}_4\text{O}_{11}$ , whereas vacancies are formed at the Zn sites. In the case of  $x < 0$  the scheme is less compatible with the structural data of Ref. 6. because of the excess in the total number of atoms in the unit cell. In order to examine the possible substitution of Zn by Ti for the case  $x > 0$  the compositional region up to  $x=0.5$  was investigated in steps of 0.05, as well as beyond this concentration up to  $x=-0.1$ .

According to the SEM micrographs and the EDX analysis of the  $\text{BaZn}_{2-2x}\text{Ti}_{4+x}\text{O}_{11}$  samples ( $0 < x < 0.5$ ), even at low  $x$  values ( $x=0.05$ ) the ceramics are not single phase: all the ceramics consist of three phases (Fig. 2a). The matrix phase has the composition of the “124” phase. The compositions of the secondary phases, which are present in minor quantities, correspond to  $\text{BaTi}_4\text{O}_9$  (dark phase) and a hollandite-type  $\text{Ba}_x\text{Zn}_x\text{Ti}_{8-x}\text{O}_{16}$  solid solution (hss) (darker phase) (Fig. 2a). With increasing  $x$  the concentration of both secondary phases increases.

In the XRD spectra the diffraction lines corresponding to the  $\text{BaTi}_4\text{O}_9$  phase only start to appear at  $x > 0.1$ ; for  $0 \leq x < 0.1$  only the diffraction lines of the “124” phase are visible (Fig. 3, curves 1 and 2). With increasing  $x$  the amount of secondary  $\text{BaTi}_4\text{O}_9$  increases; this is accompanied by the formation of another sec-

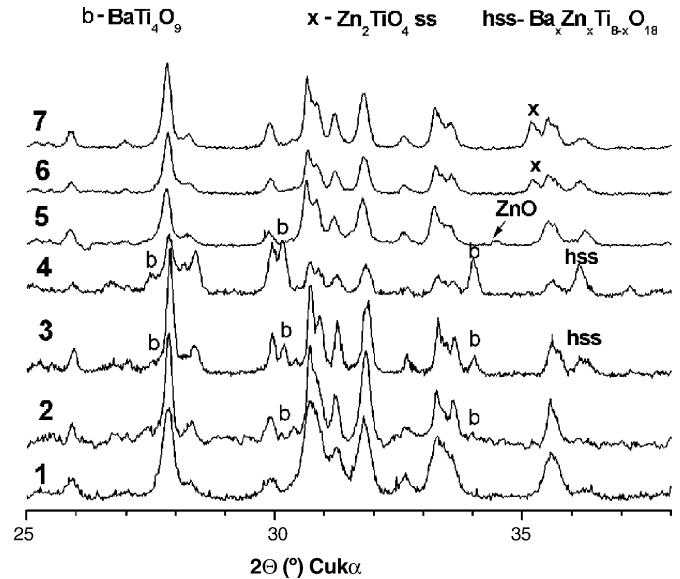


Fig. 3. XRD patterns of the ceramics: 1— $\text{BaZn}_2\text{Ti}_4\text{O}_{11}$ ; 2— $\text{BaZn}_{2-2x}\text{Ti}_{4+x}\text{O}_{11}$  ( $x=0.1$ ); 3— $\text{BaZn}_{2-2x}\text{Ti}_{4+x}\text{O}_{11}$  ( $x=0.2$ ); 4— $\text{BaZn}_{2-2x}\text{Ti}_{4+x}\text{O}_{11}$  ( $x=0.5$ ); 5— $\text{BaZn}_{2-2x}\text{Ti}_{4+x}\text{O}_{11}$  ( $x=-0.1$ ); 6— $\text{Ba}_{1-x}\text{Zn}_{2+x}\text{Ti}_4\text{O}_{11}$  ( $x=0.1$ ); 7— $\text{Ba}_{1-x}\text{Zn}_{2-x}\text{Ti}_{4+x}\text{O}_{11}$  ( $x=0.1$ ).

ondary phase of the hollandite-type  $\text{Ba}_x\text{Zn}_x\text{Ti}_{8-x}\text{O}_{18}$  solid solution (hss) (Fig. 3, curves 2–4). At  $x=0.5$  the ceramics contain almost equal quantities of  $\text{BaTi}_4\text{O}_9$ , hollandite (hss) and “124” phase (Fig. 3, curve 4).

In the case of negative  $x$  values ( $x < 0$ ) the  $\text{BaZn}_{2-2x}\text{Ti}_{4+x}\text{O}_{11}$  ceramics always display a multiphase nature in which at least two secondary phases can be detected. These phases include ZnO (light phase) as well as small inclusions of a very light phase with a composition close to  $\text{BaTi}_3\text{O}_8$  (Fig. 2b, Fig. 3, curve 5)). These phases are in accordance with the phase diagram of Ref. 6.

### 3.1.2. Scheme $\text{Ba}_{1-x}\text{Zn}_{2-x}\text{Ti}_{4+x}\text{O}_{11}$ ( $x > 0$ ; substitutional mechanism 2) and scheme $\text{BaZn}_{2-x}\text{Ti}_{4+x}\text{O}_{11+x}$ ( $x < 0$ ; substitutional mechanism 3)

This scheme implies that one Ti atom substitutes for one Zn atom for the case of  $\text{Ba}_{1-x}\text{Zn}_{2-x}\text{Ti}_{4+x}\text{O}_{11}$  ( $x > 0$ ), and vice versa for  $\text{BaZn}_{2-x}\text{Ti}_{4+x}\text{O}_{11+x}$  ( $x < 0$ ). In the former case the compensation of the charge misbalance is via the formation of vacancies at the barium sites; in the latter case ( $x < 0$ ) the charge misbalance is compensated by vacancies in the anion sublattice.

According to the EDX (Fig. 4a) and XRD results (Fig. 3, curve 7), for the substitutional mechanism  $\text{Ba}_{1-x}\text{Zn}_{2-x}\text{Ti}_{4+x}\text{O}_{11}$  ( $x > 0$ ), even at low  $x$  values the ceramics have a multiphase composition. The phases are as follows: the matrix phase (“124”), the hollandite-type solid solution hss (dark phase), and the  $\text{Zn}_2\text{TiO}_4$  ss (dark phase with darker precipitates) (Fig. 4a). Similar precipitates with the composition  $\text{Zn}_2\text{Ti}_3\text{O}_8$  were also observed in the  $\text{Zn}_2\text{TiO}_4 + 0.33\text{TiO}_2$  system at temperatures below  $945^\circ\text{C}$ .<sup>8</sup>

In the case of  $\text{BaZn}_{2-x}\text{Ti}_{4+x}\text{O}_{11+x}$  ( $x < 0$ ; substitutional mechanism 3) the phase composition of the  $\text{BaZn}_{2-x}\text{Ti}_{4+x}\text{O}_{11+x}$  ceramics is similar to that of those synthesized

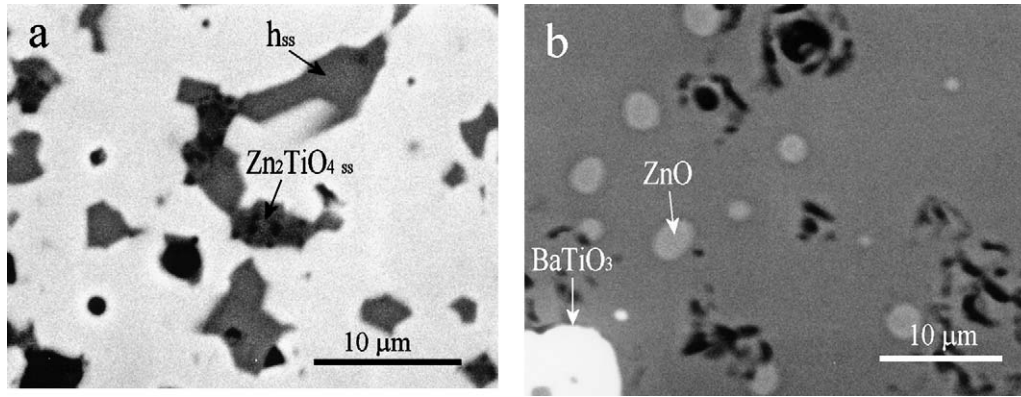


Fig. 4. SEM micrographs of the  $\text{Ba}_{1-x}\text{Zn}_{2-x}\text{Ti}_{4+x}\text{O}_{11}$  ceramics for  $x=0.05$  (a)  $\text{BaZn}_{2-x}\text{Ti}_{4+x}\text{O}_{11+x}$  for  $x=-0.1$  (b).

according to the scheme  $\text{BaZn}_{2-2x}\text{Ti}_{4+x}\text{O}_{11}$  ( $x < 0$ ). The secondary phases shown in Fig. 4 b are ZnO (light phase) and  $\text{BaTiO}_3$  (very light inclusions).

### 3.1.3. Scheme $\text{Ba}_{1-x}\text{Zn}_{2+x}\text{Ti}_4\text{O}_{11}$ (substitutional mechanism 4)

This scheme involves the substitution of Zn atoms for Ba atoms, which is rather unlikely to occur because of the big difference in the ionic radii of  $\text{Zn}^{2+}$  and  $\text{Ba}^{2+}$ . According to the experimental results this scheme always leads to a noticeable quantity of secondary phases, which can be detected by both XRD and SEM. Apart from the matrix “124” phase, a dark phase with a composition similar to the hss phase and a dark, dotted phase, with a composition corresponding to  $\text{Zn}_2\text{TiO}_4$  ss, are clearly seen in the SEM micrographs (Fig. 5). The diffraction lines corresponding to both hss and  $\text{Zn}_2\text{TiO}_4$  ss were detected on the XRD patterns collected from the  $\text{Ba}_{1-x}\text{Zn}_{2+x}\text{Ti}_4\text{O}_{11}$  ceramics, even for small substitutions (Fig. 3, curve 6). These data suggest that it is rather unlikely that Zn atoms substitute for Ba.

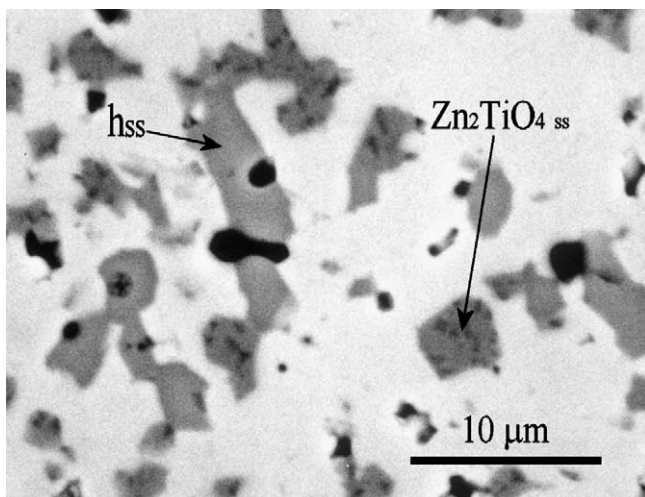


Fig. 5. SEM micrographs of the  $\text{Ba}_{1-x}\text{Zn}_{2+x}\text{Ti}_4\text{O}_{11}$  ceramics for  $x=0.1$  (substitutional mechanism 4).

### 3.1.4. Scheme $\text{BaZn}_{2-x}\text{Ti}_4\text{O}_{11-x}$ (substitutional mechanism 5)

In the case  $x > 0$  this scheme suggests the existence of vacant sites in the Zn sublattice, which are compensated by oxygen vacancies. In the case  $x < 0$  the scheme is less compatible with the structural data of Ref. 6 because of the excess of zinc and oxygen atoms with regard to the number of crystallographic sites. According to the detailed SEM and EDX investigations at low, positive  $x$  values ( $0 \leq x \leq 0.05$ ) the  $\text{BaZn}_{2-x}\text{Ti}_4\text{O}_{11-x}$  ceramics are only single phase (Fig. 6a and b). At  $x=0.1$  a small amount of the  $\text{BaTi}_4\text{O}_9$  secondary phase appears (Fig. 6c). In the case of the negative  $x$  values the ceramics always contain secondary phases, including the solid solution based on  $\text{Zn}_2\text{TiO}_4$  ss, which is detected at  $x=-0.05$ , and ZnO, which is only found at  $x=-0.1$  (Fig. 6d). Therefore, it can be stated that the homogeneity range of the “124” phase corresponds to a very narrow compositional range, described by the formula  $\text{BaZn}_{2-x}\text{Ti}_4\text{O}_{11-x}$  ( $0 < x < 0.1$ ). On the ternary phase diagram this region lies on the tie line between  $\text{BaTi}_4\text{O}_9$  and ZnO (Fig. 1).

X-ray diffraction patterns collected within the homogeneity range of the  $\text{BaZn}_{2-x}\text{Ti}_4\text{O}_{11-x}$  compound demonstrate no structural changes related to the changes in the chemical composition. The only difference involves a shift of the peaks' positions towards lower 2-theta angles with increasing Zn content (Fig. 7). These data indicate a slight increase in the unit-cell volume with increasing Zn concentration. According to the calculations performed with the help of the TOPAS R program, using full-profile fitting (space-group Pbcn, and the unit-cell parameters of  $\text{BaZn}_{2.03}\text{Ti}_{3.93}\text{O}_{10.89}$ , PDF 81-2380) the changes in the unit-cell volume are very slight (Table 1). It is evident from the table that the increase in the concentration of Zn atoms results in a slight increase in the unit cell. Since the change in the unit cell was not much more than the uncertainty (Table 1), the whole procedure from the sample preparation to the calculation of the unit-cell parameters was repeated. The scattering of the results of the calculations for the unit-cell volume of different forms of sample preparation was less than the calculated uncertainty. This proves there is a decrease in the unit-cell volume with a decrease in the Zn content within the  $\text{BaZn}_{2-x}\text{Ti}_4\text{O}_{11-x}$  ( $0 < x < 0.1$ ) homogeneity range.

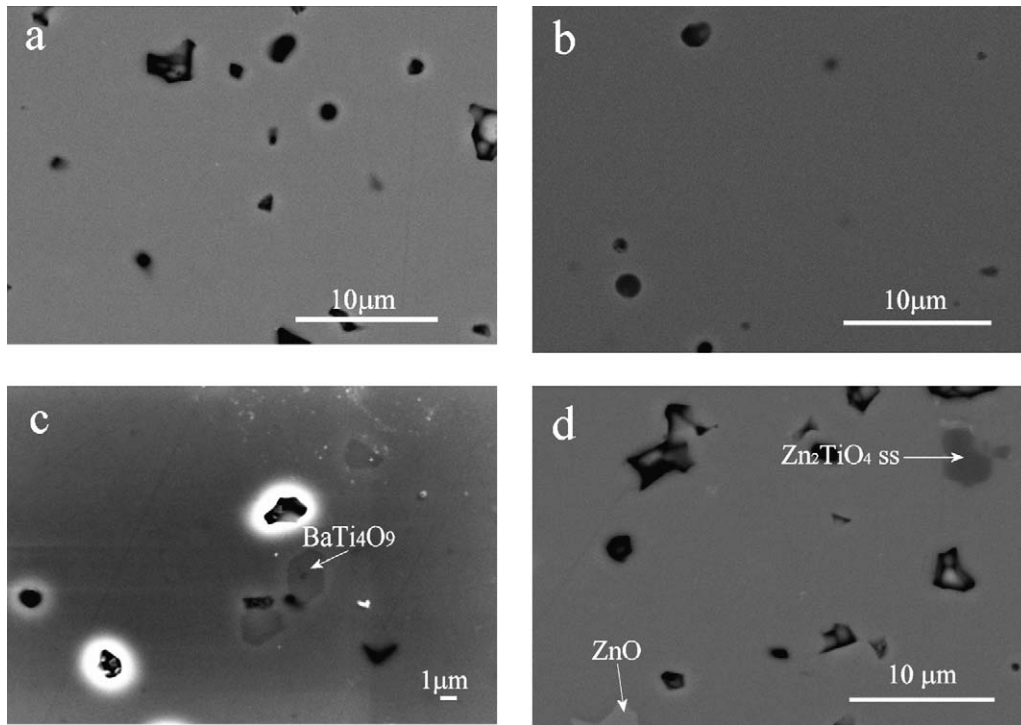


Fig. 6. SEM micrographs of the  $\text{BaZn}_{2-x}\text{Ti}_4\text{O}_{11-x}$  ceramics for  $x=0$  (a),  $x=0.05$  (b),  $x=0.1$  (c); and  $x=-0.1$  (d); (a, b and d) backscattered electrons (BE) image, (c) secondary electrons (SE) image.

### 3.2. Microwave dielectric properties of the $\text{BaZn}_2\text{Ti}_4\text{O}_{11}$ ceramics

According to the experimental results collected in the frequency range 9–11 GHz the microwave dielectric parameters ( $\epsilon$ ,  $\tau_f$ ,  $Q \times f$ ) of the investigated ceramics strongly depend on

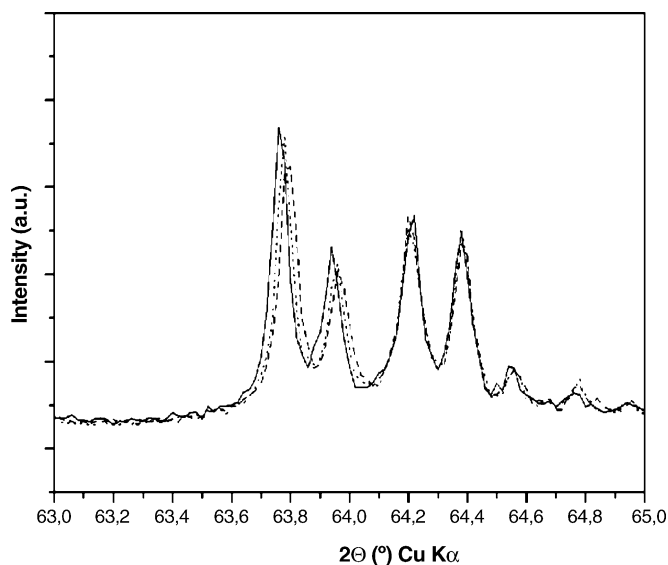


Fig. 7. Comparison between XRD spectra of the  $\text{BaZn}_2\text{Ti}_4\text{O}_{11}$  (—) and  $\text{BaZn}_{1.95}\text{Ti}_4\text{O}_{10.95}$  (...) samples sintered at  $1200^\circ\text{C}$  for 4 h and the  $\text{BaZn}_{1.95}\text{Ti}_4\text{O}_{10.95}$  (- - -) sample, which was additionally annealed at  $1100^\circ\text{C}$  for 50 h after sintering at  $1200^\circ\text{C}$  for 4 h.

their phase composition, rather than on the chemical composition of the “124” phase. The above-reported analysis of the secondary phases of the studied ceramics indicates that even a slight deviation from the “124” stoichiometry may result in a noticeable deterioration in the microwave properties. This fact is concerned mainly with the possible formation of phases like ZnO and  $\text{BaTiO}_3$ , which are known to display extremely high dielectric losses in the microwave range. Moreover, even the presence of middle-loss phases, like  $\text{Zn}_2\text{TiO}_4$ ss or hollandite-type solid solutions  $\text{Ba}_x\text{Zn}_x\text{Ti}_{8-x}\text{O}_{18}$  (hss), can affect the microwave properties significantly.<sup>1</sup> Therefore, in order to clarify the effect of secondary phases on the microwave properties of  $\text{BaZn}_2\text{Ti}_4\text{O}_{11}$ -based ceramics two cross-sections of the ternary phase diagram are analyzed below. These sections correspond to the virtual substitutional schemes  $\text{BaZn}_{2-2x}\text{Ti}_{4+x}\text{O}_{11}$  (substitutional mechanism 1) and  $\text{BaZn}_{2-x}\text{Ti}_4\text{O}_{11-x}$  (substitutional mechanism 5), and cover both the homogeneity range of the “124” phase and the field of the majority of possible secondary phases. The microwave parameters collected in these fields are summarized in Fig. 8.

According to the results presented in Fig. 8 the effects of various impurity phases on the microwave properties of the ceramics are different. Whereas an increasing content of the hollandite-type phase, which is always observed in the  $\text{BaZn}_{2-2x}\text{Ti}_{4+x}\text{O}_{11}$  ceramics with increasing  $x$ , results in an almost linear decrease in the magnitude of  $Q \times f$ , the formation of even a very small number of inclusions of high-loss ZnO and  $\text{BaTiO}_3$  in the negative  $x$  range leads to a sharp drop in the  $Q$ -factor (Fig. 8a). At the same time the presence of both  $\text{BaTi}_4\text{O}_9$  and  $\text{Zn}_2\text{TiO}_4$  ss results in a much smaller decrease in the magnitude of  $Q \times f$

Table 1  
Lattice parameters of the  $\text{BaZn}_{2-x}\text{Ti}_4\text{O}_{11-x}$  crystal phase ( $0 \leq x \leq 0.05$ )

Sample	Phase content	$a$ (Å)	$b$ (Å)	$c$ (Å)	$V$ (Å <sup>3</sup> )
BaZn <sub>1.95</sub> Ti <sub>3.9</sub> O <sub>10.95</sub> -as sintered	142	14.139(2)	11.599(1)	10.124(1)	1660.3(3)
	142	14.139(2)	11.600(1)	10.124(1)	1660.5(3)
BaZn <sub>1.95</sub> Ti <sub>3.9</sub> O <sub>10.95</sub> annealed at 1100 °C-50 h	142	14.139(2)	11.599(1)	10.122(1)	1660.2(3)
BaZn <sub>2</sub> Ti <sub>4</sub> O <sub>11</sub> -as sintered	142	14.141(2)	11.599(1)	10.127(1)	1661.2(3)
		14.142(2)	11.599(1)	10.128(1)	1661.4(3)

(Fig. 8d). An example of this fact gives us the  $Q \times f$  magnitude of the  $\text{BaZn}_{2.05}\text{Ti}_4\text{O}_{11.05}$  ceramics ( $x = -0.05$ ), which was as high as 70,000, despite the presence of the secondary  $\text{Zn}_2\text{TiO}_4$  ss phase. Another effect of the  $\text{BaTi}_4\text{O}_9$  secondary

phases and hss, which are both characterized by a positive  $\tau_f$ , is an increase in the temperature coefficient,  $\tau_f$ , with increasing  $x$  in both systems,  $\text{BaZn}_{2-2x}\text{Ti}_{4+x}\text{O}_{11}$  and  $\text{BaZn}_{2-2x}\text{Ti}_4\text{O}_{11-x}$  (Fig. 8c and f).

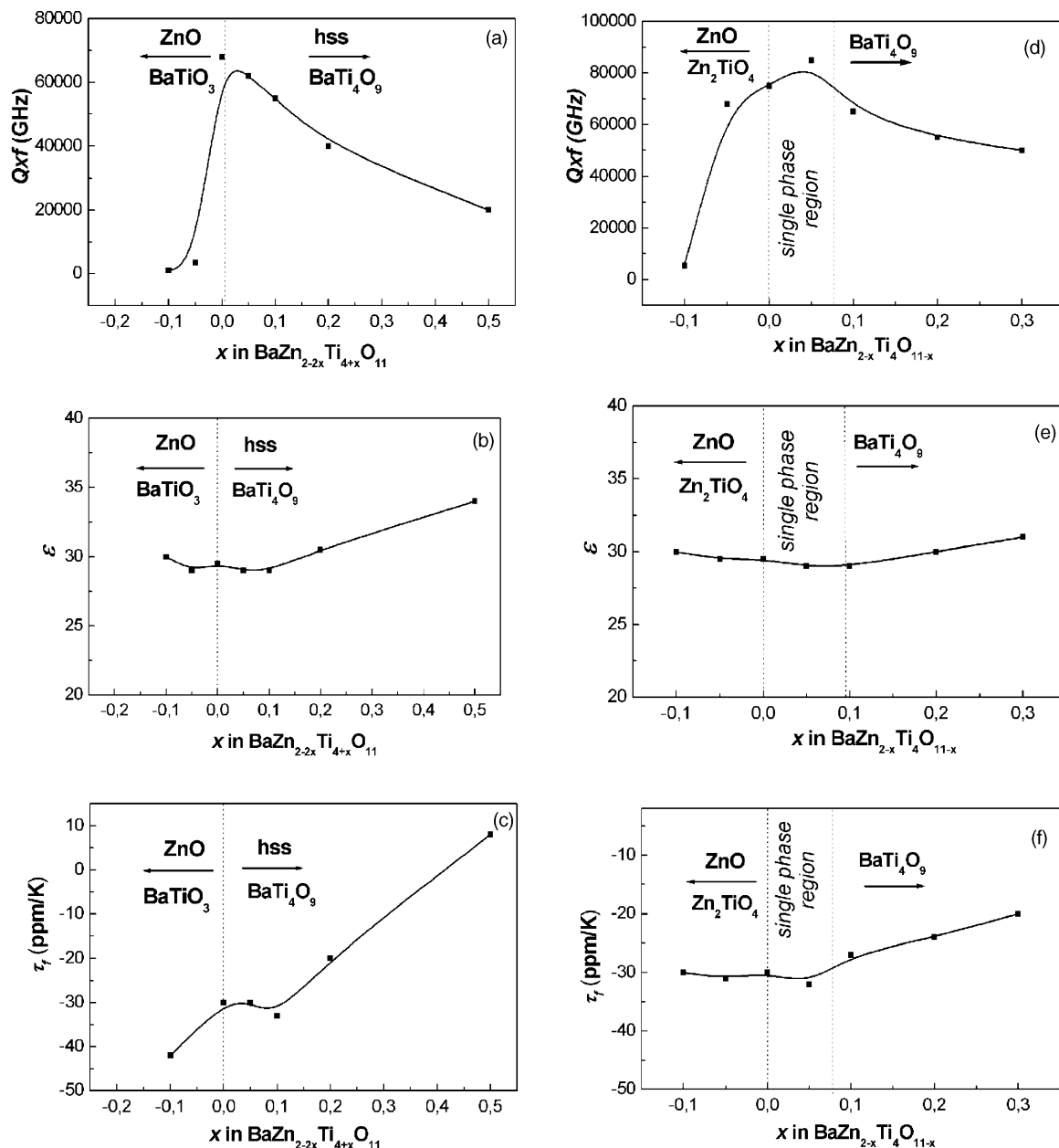


Fig. 8. Microwave dielectric properties,  $Q \times f$  (a and d),  $\epsilon$  (b and e), and  $\tau_f$  (c and f), of the ceramics with the compositions  $\text{BaZn}_{2-2x}\text{Ti}_{4+x}\text{O}_{11}$  (a–c) and  $\text{BaZn}_{2-2x}\text{Ti}_4\text{O}_{11-x}$  (d–f). Measurement frequency range: 9–11 GHz.

According to our experimental data the most prominent microwave characteristics were obtained only within the homogeneity range of  $\text{BaZn}_{2-x}\text{Ti}_4\text{O}_{11-x}$  ( $0 < x < 0.05$ ), where the  $Q \times f$  values of the single-phase materials continuously increase from values of about 65,000–70,000 at  $x = 0$  to 80,000–85,000 at  $x = 0.05$  (Fig. 8d). At the same time both the dielectric constant ( $\epsilon$ ) and the temperature coefficient of resonant frequency ( $\tau_f$ ) are practically unaffected by changes in the chemical composition in the single-phase region (Fig. 8). Within the homogeneity range the dielectric constant of  $\text{BaZn}_{2-x}\text{Ti}_4\text{O}_{11-x}$  is in the range 29–30, and  $\tau_f$  is around  $-30$  ppm/K for all values of  $x$ . The changes in both the dwell time and the heating/cooling rates do not practically affect these parameters. However, in contrast to  $\epsilon$  and  $\tau_f$ , the  $Q$ -factor of the  $\text{BaZn}_{2-x}\text{Ti}_4\text{O}_{11-x}$  phase increases when the cooling rate is low ( $0.5$ – $3.0$  °C/min). The maximum magnitude of  $Q \times f$ , about 110,000 at 10 GHz, was obtained for  $\text{BaZn}_{1.95}\text{Ti}_4\text{O}_{10.95}$  ( $x = 0.05$ ) ceramics after their slow cooling from the sintering temperature followed by an additional annealing at  $1100$  °C for 50 h. It is interesting to note that the increase in the magnitude of  $Q \times f$  was observed only in the case of the  $\text{BaZn}_{1.95}\text{Ti}_4\text{O}_{10.95}$  ( $x = 0.05$ ) ceramics, whereas prolonged high-temperature annealing of the  $\text{BaZn}_2\text{Ti}_4\text{O}_{11}$  ( $x = 0$ ) compound did not result in any significant improvement in the  $Q \times f$  values. The absence of significant structural evidence from the X-ray diffraction, which is sensitive to long-range order, indicates the possibility of short-range cation ordering, which could be the reason for the high  $Q \times f$  value of  $\text{BaZn}_{1.95}\text{Ti}_4\text{O}_{10.95}$ .

#### 4. Conclusions

According to the experimental results obtained in this study we can state that the crystal structure of  $\text{BaZn}_2\text{Ti}_4\text{O}_{11}$  (142) is formed in the homogeneity range corresponding to the formula  $\text{BaZn}_{2-x}\text{Ti}_4\text{O}_{11-x}$  ( $0 < x < 0.1$ ). Within the homogeneity range the unit-cell volume decreases with increasing  $x$ . The presence of secondary phases in the materials based on  $\text{BaZn}_2\text{Ti}_4\text{O}_{11}$

always results in deteriorating  $Q$  factors for the material: a linear decrease in the  $Q \times f$  product with an increasing content of hollandite-type solid solutions ( $\text{Ba}_x\text{Zn}_x\text{Ti}_{8-x}\text{O}_{16}$ ), and a sharp drop of  $Q$  with increasing ZnO and  $\text{BaTiO}_3$  contents. Within the homogeneity range a decrease in the unit-cell volume is accompanied by an increase in the  $Q \times f$  product. The maximum  $Q \times f$  values were obtained at  $x = 0.05$ . An increase in the cooling rate after sintering always results in a lowering of the  $Q$ -factor of the material. The highest  $Q$ -factors were obtained for single-phase materials that were additionally annealed at high temperatures. The materials based on  $\text{BaZn}_2\text{Ti}_4\text{O}_{11}$  always demonstrate a negative temperature coefficient of resonant frequency ( $\tau_f$ ) of around  $-30$  ppm/K, together with extremely high  $Q$  values. This makes them good candidates for the temperature stabilization of permittivity in various high- $Q$  microwave materials.

#### References

1. Negas, T., Yeager, G., Bell, S., Coats, N. and Minis, I.,  $\text{BaTi}_4\text{O}_9/\text{Ba}_2\text{Ti}_9\text{O}_{20}$ -based ceramics resurrected for modern microwave applications. *Am. Ceram. Soc. Bull.*, 1993, **72**, 80–89.
2. Mizuno, F. and Sato, M., *BaO-xTiO<sub>2</sub> Dielectric Ceramic Composition*, NGK Spark Plug Company, US patent 5,272,122, December 21, 1993.
3. *Dielectric Resonators*, Murata Cat. No. O95E-8.
4. Gornikov, Yu. I., Makarova, Z. Ya., Belous, A. G., Gavrilova, L. G., Paskov, V. M. and Chalyi, V. P., The effect of zinc oxide additions on the phase composition and dielectric properties of barium tetratitanate. *Sov. Prog. Chem.*, 1984, **12**(50), 1243–1245.
5. Negas, T., TransTech Inc., US patent 5,262,370, November 18, 1993.
6. Roth, R. S., Rawn, C. J., Lindsay, C. G. and Wong-Ng, W., Phase equilibria and crystal chemistry of the binary and ternary barium polytitanates and crystallography of the barium zinc polytitanates. *J. Solid State Chem.*, 1993, **104**, 99–118.
7. Ohsato, H., Nishigaki, S. and Okuda, T., Superlattice and dielectric properties of  $\text{BaO-R}_2\text{O}_{3-5}\text{TiO}_2$  ( $R = \text{La, Nd, and Sm}$ ) microwave dielectric compounds. *Jpn. J. Appl. Phys.*, 1992, **31**, 3136–3140.
8. Kim, H. T., Kim, Y., Valant, M. and Suvorov, D., Titanium Incorporation in  $\text{Zn}_2\text{TiO}_4$  Spinel Ceramics. *J. Am. Ceram. Soc.*, 2001, **84**(5), 1081–1086.
9. *Standard X-ray Diffraction Patterns*, NBS Monograph 25 12m, 1975, p. 37.